PHYSICAL REVIEW D **90,** 014031 (2014)

Diphoton production in high-energy $p + A$ collisions

Alex Kovner[1] and Amir H. Rezaeian[2,3]

[1]*Department of Physics, University of Connecticut, High, Storrs, Connecticut 06269, USA*
[2]*Departamento de Física, Universidad Técnica Federico Santa María, Avenida España 1680, Casilla 110-V Valparaiso, Chile*
[3]*Centro Científico Tecnológico de Valparaíso (CCTVal), Universidad Técnica Federico Santa María, Casilla 110-V Valparaíso, Chile*

(Received 25 April 2014; published 21 July 2014)

We consider semi-inclusive diphoton+jet and inclusive diphoton production in high-energy proton-nucleus collisions, treating the target nucleus as a color-glass condensate and the projectile proton in the parton model. We obtain the prompt diphoton production cross section in terms of fragmentation and direct contributions. The fragmentation part is given in terms of single-photon and double-photon fragmentation functions. We study prompt, direct, and fragmentation diphoton correlations in p+p and p+A collisions at the LHC and show that at low values of transverse momenta of the produced photon pair these correlations are sensitive to saturation effects. We show that back-to-back (de)correlations in prompt diphoton production are stronger in the fragmentation part than in the direct one.

DOI: 10.1103/PhysRevD.90.014031 PACS numbers: 25.75.Bh, 13.60.Hb, 13.40.-f, 25.75.Cj

I. INTRODUCTION

In recent years a lot of attention has been devoted to understanding of the physics of saturation [1]. Theoretical developments of the last 15–20 years have put this activity squarely on the first principle QCD foundations [2–6]. The saturation regime in hadronic scattering is qualitatively different from the simple parton model paradigm, and it would be extremely interesting to find clear signals of it in observed data. Its tell-tale sign is the appearance of a dimensional saturation scale in a dense system of gluons (the color-glass condensate), which should dominate many bulk observables.

Several pieces of experimental data at HERA [7–9], RHIC [10–12], and the LHC [13–21] have been indeed interpreted in the framework of saturation ideas; see also Refs. [22–25] and references therein. However, one still cannot point definitively to an experimental verification of the saturation phenomenon. It is therefore important to understand what other observables can be sensitive to saturation [26], and in particular to the existence of the saturation momentum.

One aspect of saturation that has been discussed at length in recent literature is its impact on particle correlations in the final state. This includes the effect on the ridgelike correlations in rapidity and the azimuthal angle [27–34], as well as the decorrelation effect in forward dihadron [35], photon-hadron [36,37], and Drell–Yan lepton-pair-jet [38] productions in high-energy proton-proton ($p + p$) and proton-nucleus ($p + A$) collisions. In this paper we continue the study of saturation effects on particle correlation.

The main aim of this paper is to investigate diphoton azimuthal angular correlations at forward rapidity. The mechanism of diphoton production in the color-glass condensate (CGC) saturation framework is somewhat different than that of dihadron production. Soft gluons are scattered out of the projectile wave function by directly scattering on a saturated target and via subsequent hadronization produce hadrons. Photons, on the other hand, do not scatter themselves but rather decohere from the scattered quarks. It is thus interesting to see whether saturation has any discernible effects on the correlations between produced photons.

In terms of theoretical description, there are clear advantages to studying prompt diphoton production as compared to dihadron production. For final-state photons, the difficulties involved with description of hadronization of final-state quarks and gluons do not arise. For hadronic final states, this stage of the process is usually described in terms of fragmentation functions, and this description is valid only at high transverse momentum. Additionally, one does not need to be concerned with possible initial-state–final-state interference effects which are present for hadron production. Within the CGC framework, the theoretical understanding of observables necessary to describe diphoton production is more robust. Unlike the description of dihadron correlations, which necessitates the knowledge of correlators of a higher number of Wilson lines, the diphoton production cross section depends only on the dipole amplitude, which is the best understood observable in terms of high-energy evolution.

The diphoton production in proton-proton and antiproton-proton collisions has been intensively investigated in the literature; see, for example, Refs. [39–41]. Precise theoretical understanding of the diphoton production in the standard model provides valuable guidance for the Higgs boson signal [42]. In the present paper, for the first time, we investigate diphoton production in high-energy proton-nucleus collisions. We obtain the prompt diphoton cross

section in the leading logarithmic approximation in terms of fragmentation and direct contributions, where the fragmentation part is given in terms of single-photon and double-photon fragmentation functions. We show that at low values of transverse momenta of the produced photon pair back-to-back (de)correlations in diphoton production are stronger in the fragmentation part than in the direct one.

The plan of this paper is the following. In Sec. II we derive the basic formulas for calculating the cross section of semi-inclusive diphoton + jet and inclusive diphoton production in high-energy proton-proton and proton-nucleus collisions in the CGC framework. The CGC approach is a first-principle effective field theory approach that describes the high-energy limit of QCD. In this formalism quantum corrections enhanced by large logarithms of $1/x$ are systematically resummed incorporating high gluon density effects at small x and for large nuclei [2–4]. In Sec. II we also discuss the soft limit, in which the expressions simplify and become amenable to numerical calculations. As an illustrative example, in Sec. II, we also obtain the cross section of single inclusive prompt photon production in the soft approximation. In Sec. III we present the results of numerical calculations for correlations in direct, fragmentation, and prompt diphoton production, together with a short discussion. We summarize our main results in Sec. IV.

II. SEMI-INCLUSIVE DIPHOTON+JET PRODUCTION IN PROTON-NUCLEUS COLLISIONS

In this section we introduce the basic formulas for calculating the cross section for the process $h + A \to \gamma_1 + \gamma_2 + X$, where a dilute projectile hadron interacts coherently with a dense target A and produces two photons γ_1 and γ_2. In the leading-order approximation, at forward rapidity, a valence quark of the projectile hadron emits two photons via bremsstrahlung, and the produced diphoton + jet is then put on shell by interacting coherently over the whole longitudinal extent of the target. The cross section for production of a quark with momentum q and two prompt photons with momenta k_1 and k_2 in the scattering of an on-shell quark with momentum p off a hadronic target (either a proton or a nucleus),

$$q(p) + A \to \gamma(k_1) + \gamma(k_2) + \mathrm{jet}(q) + X, \tag{1}$$

can be written in the general form

$$d\sigma^{q\to q\gamma\gamma} = \frac{d^3k_1}{(2\pi)^3 2k_1^-}\frac{d^3k_2}{(2\pi)^3 2k_2^-}\frac{d^3q}{(2\pi)^3 2q^-}\frac{1}{2p^-}(2\pi)|\mathcal{M} \times (p|q,k_1,k_2)|^2\delta(p^- - q^- - k_1^- - k_2^-), \tag{2}$$

where the matrix element $\mathcal{M}$ is related to the scattering amplitude by

$$\langle q(q),\gamma(k_1),\gamma(k_2)|q(p)\rangle = (2\pi)\delta(p^- - q^- - k_1^- - k_2^-)\mathcal{M}(p|q,k_1,k_2). \tag{3}$$

In the CGC approach, we assume that the small-x gluon modes of the nucleus have a large occupation number so that it can be described in terms of a classical color field. This should be a good approximation for large enough nucleus at high energy.[1] This color field emerges from the classical Yang–Mills equation with a source term provided by faster partons. The renormalization group equations which govern the separation between the soft and hard models are then given by the nonlinear Jalilian-Marian, Iancu, McLerran, Weigert, Leonidov, and Kovner (JIMWLK) evolution equations [3] (see below). We further assume that the projectile proton is in the dilute regime and can be described in the ordinary perturbative approach, in terms of parton distribution functions. In this framework, the scattering amplitude of diphoton + jet production in quark-nucleus scatterings in momentum space in lowest order in the electromagnetic α_{em} and the strong α_s coupling constants can be written in the formal form

$$\begin{aligned}\langle q(\mathbf{q}),\gamma(\mathbf{k}_1),\gamma(\mathbf{k}_2)|q(\mathbf{p})\rangle &= -ie_q^2\bar{u}(\mathbf{q})[\mathcal{T}_F(q;p-k_1-k_2)G_F^0(p-k_1-k_2)\\ &\times \not{\epsilon}(k_2)G_F^0(p-k_1)\not{\epsilon}(k_1) + \not{\epsilon}(k_2)G_F^0(q+k_2)\not{\epsilon}(k_1)\\ &\times G_F^0(q+k_1+k_2)\mathcal{T}_F(q+k_1+k_2;p) + \not{\epsilon}(k_2)\\ &\times G_F^0(q+k_2)\mathcal{T}_F(q+k_2;p-k_1)G_F^0(p-k_1)\not{\epsilon}(k_1)\\ &+ (k_1\leftrightarrow k_2)]u(\mathbf{p}),\end{aligned} \tag{4}$$

where e_q is the fractional electric charge of the projectile quark, G_F^0 is the free Feynman propagator of a quark, and u and ϵ_μ denote the quark free spinor and the photon polarization vector, respectively. In the above, the operator matrix $\mathcal{T}_F$ contains the interaction between the quark and the colored-glass condensate target, which resums multiple interactions with the background CGC field [43,44]. Assuming that the target is moving in the positive z direction, we have [45]

$$\mathcal{T}_F(q;p) = 2\pi\delta(q^- - p^-)\gamma^-\mathrm{sign}(p^-) \times \int d^2\mathbf{z_T}[U(\mathbf{z_T}) - 1]e^{i(\mathbf{q_T}-\mathbf{p_T})\cdot\mathbf{z_T}}, \tag{5}$$

where $U(z_T)$ is a unitary matrix in the fundamental representation of $SU(N_c)$—the scattering matrix of a quark on the colored-glass condensate target:

$$U(\mathbf{z_T}) = T\exp\left(-ig^2\int dx^-\frac{1}{\nabla_T^2}\rho_a(x^-,\mathbf{x_T})t^a\right). \tag{6}$$

[1]Note that proton at high energy and specially at very forward rapidity is a dense system, and in principle the same approximation also applies there; see, for example, Refs. [7–21].

Here ρ is the density of the color sources in the target, and t^a is the generator of $SU(N_c)$ in the fundamental representation. The expression in Eq. (4) accounts for all processes illustrated in Fig. 1 for diphoton+jet production of a quark interacting with the CGC background field at lowest order in α_{em} and α_s in the leading-log approximation. Note that the lower diagram on the right panel in Fig. 1 does not contribute at high energy. Conceptually this is because the nucleus is moving with speed of light in the $+z$ direction. By the time the diphoton is emitted from the quark, the nucleus has already moved far away from the quark, and no further interactions are allowed by causality.

Using the definition of $\mathcal{T}_F$ in Eq. (5), one can rewrite the amplitude as

$$\begin{aligned}\langle q(\mathbf{q}),\gamma(\mathbf{k}_1),\gamma(\mathbf{k}_2)|q(\mathbf{p})\rangle = ie_q^2\bar{u}(\mathbf{q})\Bigg[&\frac{\gamma^-(\not p-\not k_1-\not k_2)\not\epsilon(k_2)(\not p-\not k_1)\not\epsilon(k_1)}{(p-k_1-k_2)^2(p-k_1)^2}+\frac{\not\epsilon(k_2)(\not q+\not k_2)\not\epsilon(k_1)(\not q+\not k_1+\not k_2)\gamma^-}{(q+k_2)^2(q+k_1+k_2)^2}\\&+\frac{\not\epsilon(k_2)(\not q+\not k_2)\gamma^-(\not p-\not k_1)\not\epsilon(k_1)}{(q+k_2)^2(p-k_1)^2}+(k_1\leftrightarrow k_2)\Bigg]u(\mathbf{p})\\&\times 2\pi\delta(q^-+k_1^-+k_2^--p^-)\int d^2\mathbf{z_T}[U(\mathbf{z_T})-1]e^{i(\mathbf{q_T}+\mathbf{k_{1T}}+\mathbf{k_{2T}}-\mathbf{p_T})\cdot\mathbf{z_T}}.\end{aligned}\tag{7}$$

The semi-inclusive diphoton + jet cross section defined in Eq. (2) can be readily obtained by squaring the amplitude and averaging over the color charge distribution. To this end, one needs to perform the color charge averaging of the expression $\langle U^\dagger(\mathbf{x_T})U(\mathbf{y_T})\rangle_\rho$ with the CGC weight

$$W[\rho]=T\exp\left(-\int dx^-d^2\mathbf{x_T}\frac{\rho_a(x^-,\mathbf{x_T})\rho^a(x^-,\mathbf{x_T})}{2\mu^2(x^-)}\right).\tag{8}$$

Note that the averaging procedure does not affect the spin dependence in Eq. (2). Therefore, one can rewrite the final expression in term of the dipole-target forward scattering amplitude N_F and a spin trace,

$$\begin{aligned}d\sigma^{q\to q\gamma\gamma}=&\frac{e_q^4}{2}\frac{d^3\mathbf{k}_1}{(2\pi)^3 2k_1^-}\frac{d^3\mathbf{k}_2}{(2\pi)^3 2k_2^-}\frac{d^3\mathbf{q}}{(2\pi)^3 2q^-}\frac{1}{2p^-}(2\pi)\delta(p^--q^--k_1^--k_2^-)\langle\mathrm{tr}(S^\dagger S)\rangle_{\mathrm{spin}}\\&\times d^2\mathbf{r_T}d^2\mathbf{b_T}e^{i(\mathbf{p_T}-\mathbf{q_T}-\mathbf{k_{1T}}-\mathbf{k_{2T}})\cdot\mathbf{r_T}}N_F(\mathbf{b_T},\mathbf{r_T},x_g),\end{aligned}\tag{9}$$

where the factor $1/2$ is due to averaging over flavor SU(2) and N_F is the imaginary part of the (quark-antiquark) dipole-target forward scattering amplitude defined as

$$N_F(\mathbf{b_T},\mathbf{r_T},x_g)=\frac{1}{N_c}\langle\mathrm{Tr}[1-U^\dagger(\mathbf{x_T})U(\mathbf{y_T})]\rangle.\tag{10}$$

Here N_c is the number of colors, the vector $\mathbf{b_T}\equiv(\mathbf{x_T}+\mathbf{y_T})/2$ is the impact parameter of the dipole relative to the target, and $\mathbf{r_T}\equiv\mathbf{x_T}-\mathbf{y_T}$ is the dipole transverse vector. The dependence of the dipole scattering probability on Bjorken x_g is determined by the JIMWLK renormalization group equations (see Sec. III). The explicit expression for the trace in Eq. (3) is

$$\begin{aligned}\langle\mathrm{tr}(S^\dagger S)\rangle_{\mathrm{spin}}=\frac{1}{2}\,\mathrm{tr}\Bigg\{&\not p\Bigg[\frac{\not\epsilon^*(k_1)(\not p-\not k_1)\not\epsilon^*(k_2)(\not p-\not k_1-\not k_2)\gamma^-}{(p-k_1-k_2)^2(p-k_1)^2}+\frac{\gamma^-(\not q+\not k_1+\not k_2)\not\epsilon^*(k_1)(\not q+\not k_2)\not\epsilon^*(k_2)}{(q+k_2)^2(q+k_1+k_2)^2}\\&+\frac{\not\epsilon^*(k_1)(\not p-\not k_1)\gamma^-(\not q+\not k_2)\not\epsilon^*(k_2)}{(q+k_1)^2(p-k_2)^2}+\frac{\not\epsilon^*(k_2)(\not p-\not k_2)\not\epsilon^*(k_1)(\not p-\not k_1-\not k_2)\gamma^-}{(p-k_1-k_2)^2(p-k_2)^2}\\&+\frac{\gamma^-(\not q+\not k_1+\not k_2)\not\epsilon^*(k_2)(\not q+\not k_1)\not\epsilon^*(k_1)}{(q+k_1)^2(q+k_1+k_2)^2}+\frac{\not\epsilon^*(k_2)(\not p-\not k_2)\gamma^-(\not q+\not k_1)\not\epsilon^*(k_1)}{(q+k_2)^2(p-k_1)^2}\Bigg]\\&\times\not q\Bigg[\frac{\gamma^-(\not p-\not k_1-\not k_2)\not\epsilon(k_2)(\not p-\not k_1)\not\epsilon(k_1)}{(p-k_1-k_2)^2(p-k_1)^2}+\frac{\not\epsilon(k_2)(\not q+\not k_2)\not\epsilon(k_1)(\not q+\not k_1+\not k_2)\gamma^-}{(q+k_2)^2(q+k_1+k_2)^2}\\&+\frac{\not\epsilon(k_2)(\not q+\not k_2)\gamma^-(\not p-\not k_1)\not\epsilon(k_1)}{(q+k_2)^2(p-k_1)^2}+\frac{\gamma^-(\not p-\not k_1-\not k_2)\not\epsilon(k_1)(\not p-\not k_2)\not\epsilon(k_2)}{(p-k_1-k_2)^2(p-k_2)^2}\\&+\frac{\not\epsilon(k_1)(\not q+\not k_1)\not\epsilon(k_2)(\not q+\not k_1+\not k_2)\gamma^-}{(q+k_1)^2(q+k_1+k_2)^2}+\frac{\not\epsilon(k_1)(\not q+\not k_1)\gamma^-(\not p-\not k_2)\not\epsilon(k_2)}{(q+k_1)^2(p-k_2)^2}\Bigg]\Bigg\},\end{aligned}\tag{11}$$

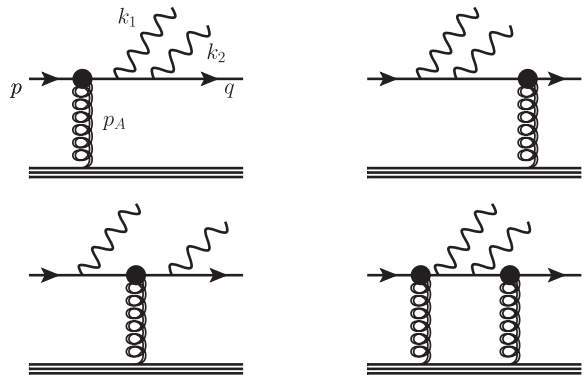

FIG. 1. The diagrams contributing to diphoton production of a quark in the background of the CGC field. The black blob denotes the interaction of a quark to all orders with the background field via multiple gluon exchanges. See the Appendix for the definition of kinematics.

where the factor $1/2$ is due to averaging over the spin of the projectile quark. The trace in Eq. (11) can be somewhat simplified by summing over the photon polarization and using the relation $\epsilon_\mu(\mathbf{k})\epsilon^*_\nu(\mathbf{k}) = -g_{\mu\nu}$ (note that terms proportional to k_μ do not contribute due to Ward identities). Moreover, half of the terms in Eq. (11) are symmetric under the replacement of $k_1 \to k_2, k_2 \to k_1$. Nevertheless, even after these simplifications, the exact expression for the trace in Eq. (11) is rather complicated and very difficult for a numerical evaluation. However, one can simplify it significantly by restricting to the soft limit, which is relevant for the high-energy collisions (see below).

A. Single-inclusive prompt photon production: Soft limit

The calculation of the photon + jet and diphoton + jet production in the CGC approach in the soft limit is rather similar. Therefore, it is instructive to first derive the cross section of semi-inclusive photon + jet production.

Let us consider production of a single prompt photon and a quark with 4-momenta k and q, respectively, in scattering of a on-shell quark with 4-momentum p on a nuclear (or proton) target in the CGC approach in the soft approximation, namely, when $|k| < |p-q|$. To this end, one can calculate the amplitude from diagrams similar to those shown in the upper panel of Fig. 1 replacing two photon lines by a single one with momentum k [45]:

$$\langle q(\mathbf{q}),\gamma(\mathbf{k})|q(\mathbf{p})\rangle = -ie_q\bar{u}(\mathbf{q})\left[\frac{\gamma^-(\not{p}-\not{k})\not{\epsilon}}{(p-k)^2}+\frac{\not{\epsilon}(\not{q}+\not{k})\gamma^-}{(q+k)^2}\right]u(\mathbf{p})2\pi\delta(q^-+k^--p^-)\int d^2\mathbf{z}_T[U(\mathbf{z}_T)-1]e^{i(\mathbf{q}_T+\mathbf{k}_T-\mathbf{p}_T)\cdot\mathbf{z}_T},$$
$$\approx -ie_q\bar{u}(\mathbf{q})\gamma^-u(\mathbf{p})\left[\frac{q\cdot\epsilon}{q\cdot k}-\frac{p\cdot\epsilon}{p\cdot k}\right]2\pi\delta(q^-+k^--p^-)\int d^2\mathbf{z}_T[U(\mathbf{z}_T)-1]e^{i(\mathbf{q}_T+\mathbf{k}_T-\mathbf{p}_T)\cdot\mathbf{z}_T}. \quad (12)$$

In the above equation's second line, we implemented the soft limit approximation and used

$$\not{p}\not{\epsilon}u(\mathbf{p}) = 2p\cdot\epsilon u(\mathbf{p}), \qquad \bar{u}(\mathbf{q})\not{\epsilon}\not{q} = \bar{u}(\mathbf{q})2q\cdot\epsilon, \qquad (p-k)^2 \approx -2p\cdot k. \quad (13)$$

The spinor averaged matrix element can be then immediately obtained,

$$\langle \mathrm{tr}(S^\dagger S)\rangle^{\text{single-photon,soft}}_{\text{spin}} = \frac{1}{2}\,\mathrm{tr}\{\not{q}\gamma^-\not{p}\gamma^-\}\left|\frac{q\cdot\epsilon(k)}{q\cdot k}-\frac{p\cdot\epsilon(k)}{p\cdot k}\right|^2 = 16p^-q^-\left[\frac{(p\cdot q)}{(q\cdot k)(p\cdot k)}\right], \quad (14)$$

$$= \frac{32p^-q^-k^{-2}\mathbf{q}_T^2}{\mathbf{k}_T^2(k^-\mathbf{q}_T-q^-\mathbf{k}_T)^2}. \quad (15)$$

In Eq. (14) summations over the spin of the final quark and over the polarization of the photon were performed. The cross section of single inclusive prompt photon production, similar to Eq. (9), can be written as

$$d\sigma^{q\to q\gamma} = \frac{e_q^2}{2}\frac{d^3\mathbf{k}}{(2\pi)^3 2k^-}\frac{d^3\mathbf{q}}{(2\pi)^3 2q^-}\frac{1}{2p^-}(2\pi)\delta(p^--q^--k^-)\langle \mathrm{tr}(S^\dagger S)\rangle^{\text{single-photon}}_{\text{spin}} d^2\mathbf{r}_T d^2\mathbf{b}_T e^{i(\mathbf{p}_T-\mathbf{q}_T-\mathbf{k}_T)\cdot\mathbf{r}_T}N_F(\mathbf{b}_T,\mathbf{r}_T,x_g). \quad (16)$$

Using Eq. (15) and the definitions of the rapidities of the produced photon $\eta_\gamma = \log(\frac{\sqrt{2}k^-}{k_T})$ and quark $\eta_h = \log(\frac{\sqrt{2}q^-}{q_T})$, the above equation can be simplified in the soft limit to yield

$$\frac{d\sigma^{q(p)\to q(q)\gamma(k)X}}{dk_T^2 d\eta_\gamma dq_T^2 d\eta_h d\theta} = \frac{2\alpha_{em}e_q^2}{(2\pi)^3\sqrt{2s}}\frac{q^- k^{-2} q_T^2}{k_T^2(k^-\mathbf{q}_T - q^-\mathbf{k}_T)^2}\delta\left(x_q - \frac{k_T}{\sqrt{s}}e^{\eta_\gamma} - \frac{q_T}{\sqrt{s}}e^{\eta_h}\right) \times \int d^2\mathbf{r}_T d^2\mathbf{b}_T e^{i(\mathbf{q}_T+\mathbf{k}_T).\mathbf{r}_T} N_F(\mathbf{b}_T, \mathbf{r}_T, x_g), \tag{17}$$

where θ is the angle between the produced jet and photon. The parameter x_q is the ratio of energies of the incoming quark to nucleon, $x_q = p^-/\sqrt{s/2}$ with $\sqrt{s}$ being the nucleon-nucleon center-of-mass energy.

To relate the above partonic production cross section to the cross section of photon-hadron production in proton-nucleus collisions, one needs to convolute the partonic cross section with the quark and antiquark distribution functions of a proton and the quark-hadron fragmentation function,

$$\frac{d\sigma^{q(p)\to h(q')\gamma(k)}}{d^2\mathbf{k}_T d\eta_\gamma d^2\mathbf{q}_T' d\eta_h d\theta} = \int_{z_h^{\min}}^1 \frac{dz_h}{z_h^2}\int dx_q f(x_q,\mu_I^2) \times \frac{d\sigma^{q(p)\to q(q)\gamma(k)}}{d^2\mathbf{k}_T d\eta_\gamma d^2\mathbf{q}_T d\eta_h d\theta} \times D_{h/q}(z_h,\mu_F^2), \tag{18}$$

where q_T' is the transverse momentum of the produced hadron and $f(x_q,\mu_I^2)$ is the parton distribution function (PDF) of the incoming proton, which depends on the light-cone momentum fraction x_q and the hard-scale μ_I. Summation over the quark and antiquark flavors in the above expression is understood. The function $D_{h/q}(z_f,\mu_F^2)$ is the quark-hadron fragmentation function (FF) where z_h is the ratio of energies of the produced hadron and quark and μ_F is the fragmentation scale. The produced hadrons are assumed here to be massless. The light-cone momentum fractions x_q, x_g, z_h are related to the transverse momenta and rapidities of the produced hadron and prompt photon via

$$\begin{aligned} x_q &= x_{\bar{q}} = \frac{1}{\sqrt{s}}\left(k_T e^{\eta_\gamma} + \frac{q_T'}{z_h}e^{\eta_h}\right), \\ x_g &= \frac{1}{\sqrt{s}}\left(k_T e^{-\eta_\gamma} + \frac{q_T'}{z_h}e^{-\eta_h}\right), \\ z_h &= q_T'/q_T \quad \text{with} \quad z_h^{\min} = \frac{q_T'}{\sqrt{s}}\left(\frac{e^{\eta_h}}{1-\frac{k_T}{\sqrt{s}}e^{\eta_\gamma}}\right). \end{aligned} \tag{19}$$

To obtain the cross section for the single inclusive prompt photon production, we integrate over the outgoing quark momentum in Eq. (17). Using $d\eta_h = dq^-/q^-$ we obtain

$$\frac{d\sigma^{q(p)\to\gamma(k)X}}{d^2\mathbf{k}_T d\eta_\gamma} = \frac{2\alpha_{em}e_q^2}{(2\pi)^3 k_T^2}\int d^2\mathbf{q}_T \frac{k^{-2}\mathbf{q}_T^2}{(k^-\mathbf{q}_T - q^-\mathbf{k}_T)^2} \times N_F(|\mathbf{q}_T+\mathbf{k}_T|, x_g). \tag{20}$$

In terms of the photon fragmentation parameter $z = k^-/p^-$, the light-cone fraction variable x_g in Eq. (20) is then expressed as

$$x_g = \frac{1}{x_q s}\left[\frac{k_T^2}{z} + \frac{q_T^2}{1-z}\right]. \tag{21}$$

The collinear singular part in Eq. (20) is naturally attributed to the fragmentation contribution. Shifting the momentum $\mathbf{q}_T \to \mathbf{q}_T + \mathbf{k}_T/z$ and breaking the integral into two parts by introducing a hard cutoff, the cross section of the single inclusive prompt photon can be written as a sum of the fragmentation and the direct photon (finite) part,

$$\frac{d\sigma^{q(p)\to\gamma(k)X}}{d^2\mathbf{k}_T d\eta_\gamma} = \frac{\alpha_{em}e_q^2}{\pi(2\pi)^3}\frac{2}{k_T^2}\int_{q_T^2>\mu_F^2} d^2\mathbf{q}_T \frac{|\mathbf{q}_T+\mathbf{k}_T/z|^2}{q_T^2} \times N_F(|\mathbf{q}_T+\mathbf{k}_T(1+1/z)|, x_{1g}) + \frac{1}{(2\pi)^2}\frac{1}{z}D_{\gamma/h}(z,\mu_F^2)N_F(k_T/z, x_{2g}), \tag{22}$$

where the fragmentation scale μ_F used to separate the soft from the hard contribution. The first term is the direct photon contribution, whereas the second term is the fragmentation photon contribution, corresponding to the kinematics where the photon is emitted almost collinearly with the outgoing quark. The photon fragmentation function extracted from Eq. (20) in the soft approximation is given by

$$D_{\gamma/h}(z,\mu_F^2) = \frac{\alpha_{em}e_q^2}{2\pi}\frac{2}{z}\log(\mu_F^2/\Lambda_{QCD}^2). \tag{23}$$

The light-cone fraction variables x_{1g} and x_{2g} in Eq. (22) are obtained via Eq. (21) by replacing $\mathbf{q}_T \to \mathbf{q}_T + \mathbf{k}_T/z$ and $\mathbf{q}_T \to \mathbf{k}_T/z$, respectively. The above expression for the single-inclusive photon fragmentation function agrees with the corresponding expression obtained in the standard perturbative QCD calculation in the leading-log approximation in the soft limit [36,46]. Note that in the soft photon approximation we assumed $z \ll 1$ and $k_T \ll q_T$. The cross section given in Eq. (22) is also in accordance with expression obtained in Refs. [36,45,47] in the soft limit.

Note that both the direct and fragmentation cross section for single inclusive photon production are explicitly proportional to the dipole amplitude. Thus, in principle they probe the small-x dynamics and saturation physics in the appropriate kinematics [36,37] (see also Ref. [48]).

B. Semi-inclusive diphoton + jet production: Soft limit

We now turn to the problem of diphoton + jet production in proton-nucleus collisions assuming that the radiated photons are soft, namely, $|k_{1,2}| < |p-q|$. In this case we can simplify the expression in Eq. (7) by ignoring $\not{k}_{1,2}$ in the numerators of the propagator and using similar relations given in Eq. (13). In the soft-photon approximation, the amplitude of diphoton + jet production in quark-nucleus collisions becomes

$$\langle q(\mathbf{q}),\gamma(\mathbf{k}_1),\gamma(\mathbf{k}_2)|q(\mathbf{p})\rangle \approx ie_q^2\bar{u}(\mathbf{q})\left[\frac{\gamma^- p\cdot\epsilon(k_2)p\cdot\epsilon(k_1)}{p\cdot(k_1+k_2)(p\cdot k_1)}+\frac{\gamma^- q\cdot\epsilon(k_2)q\cdot\epsilon(k_1)}{(q\cdot k_2)q\cdot(k_1+k_2)}-\frac{\gamma^- q\cdot\epsilon(k_2)p\cdot\epsilon(k_1)}{(q\cdot k_2)(p\cdot k_1)}+(k_1\leftrightarrow k_2)\right]u(\mathbf{p})$$
$$\times 2\pi\delta(q^-+k_1^-+k_2^--p^-)\int d^2\mathbf{z}_T[U(\mathbf{z_T})-1]e^{i(\mathbf{q}_T+\mathbf{k}_{1T}+\mathbf{k}_{2T}-\mathbf{p}_T)\cdot\mathbf{z}_T}. \tag{24}$$

Using the above expression for the amplitude, after some algebra one can significantly simplify the spinor trace in Eq. (11) to obtain

$$\begin{aligned}\langle \mathrm{tr}(S^\dagger S)\rangle_{\mathrm{spin}}^{\mathrm{diphoton,\ soft}} &= \frac{1}{2}\mathrm{tr}\{\not{q}\gamma^-\not{p}\gamma^-\}\left|\frac{p\cdot\epsilon(k_2)p\cdot\epsilon(k_1)}{p\cdot(k_1+k_2)(p\cdot k_1)}+\frac{q\cdot\epsilon(k_2)q\cdot\epsilon(k_1)}{(q\cdot k_2)q\cdot(k_1+k_2)}-\frac{q\cdot\epsilon(k_2)p\cdot\epsilon(k_1)}{(q\cdot k_2)(p\cdot k_1)}+(k_1\leftrightarrow k_2)\right|^2,\\ &= \mathrm{tr}\{\not{q}\gamma^-\not{p}\gamma^-\}(p\cdot q)^2\left[\frac{1}{p\cdot(k_1+k_2)(p\cdot k_1)(q\cdot k_2)q\cdot(k_1+k_2)}\right.\\ &\quad+\frac{1}{p\cdot(k_1+k_2)(p\cdot k_1)(q\cdot k_1)q\cdot(k_1+k_2)}+\frac{1}{(q\cdot k_2)q\cdot(k_1+k_2)p\cdot(k_1+k_2)(p\cdot k_2)}\\ &\quad\left.+\frac{1}{(q\cdot k_1)q\cdot(k_1+k_2)p\cdot(k_1+k_2)(p\cdot k_2)}+\frac{1}{(q\cdot k_2)(p\cdot k_1)(q\cdot k_1)(p\cdot k_2)}\right],\\ &= 64p^-q^-k_1^{-2}k_2^{-2}q_T^4\left[\frac{k_1^-k_2^-}{\mathcal{O}M}\left(\frac{1}{k_{1T}^2D(k_2)}+\frac{1}{k_{2T}^2D(k_1)}\right)+\frac{1}{\mathcal{O}M}\left(\frac{k_1^{-2}}{k_{1T}^2D(k_1)}+\frac{k_2^{-2}}{k_{2T}^2D(k_2)}\right)\right.\\ &\quad\left.+\frac{1}{k_{1T}^2k_{2T}^2D(k_1)D(k_2)}\right],\end{aligned} \tag{25}$$

where we introduced the notation

$$\begin{aligned}D(k_i) &= (k_i^-\mathbf{q}_T-q^-\mathbf{k}_{iT})^2 \quad \text{with} \quad i=1,2,\\ M &= k_2^-D(k_1)+k_1^-D(k_2),\\ \mathcal{O} &= k_{1T}^2k_2^-+k_{2T}^2k_1^-,\end{aligned} \tag{26}$$

with k_1^-, k_2^-, and q^- being related to the transverse momenta and pseudorapidities of the produced diphoton $\eta_{\gamma_1},\eta_{\gamma_2}$ and the jet η_h via

$$k_1^- = \frac{k_{1T}}{\sqrt{2}}e^{\eta_{\gamma_1}}, \qquad k_2^- = \frac{k_{2T}}{\sqrt{2}}e^{\eta_{\gamma_2}}, \qquad q^- = \frac{q_T}{\sqrt{2}}e^{\eta_h}. \tag{27}$$

In the last line of Eq. (25), we explicitly used the kinematical relations between the 4-momenta of the produced photons and the jet in the light-cone frame arising due to energy-momentum conservation (see the Appendix). Substituting the above expression into Eq. (9), the diphoton + jet cross-section at partonic level in quark-nucleus collisions can be simplified to

$$\begin{aligned}\frac{d\sigma^{qA\to q(q)\gamma(k_1)\gamma(k_2)X}}{d^2\mathbf{k}_{1T}d\eta_{\gamma_1}d^2\mathbf{k}_{2T}d\eta_{\gamma_2}d^2\mathbf{q}_Td\eta_h} &= \frac{4\alpha_{em}^2e_q^4}{(2\pi)^6\sqrt{2s}}q^-k_1^{-2}k_2^{-2}q_T^4\delta\left(x_q-\frac{k_{1T}}{\sqrt{s}}e^{\eta_{\gamma_1}}-\frac{k_{2T}}{\sqrt{s}}e^{\eta_{\gamma_2}}-\frac{q_T}{\sqrt{s}}e^{\eta_h}\right)\\ &\quad\times\left[\frac{k_1^-k_2^-}{\mathcal{O}M}\left(\frac{1}{k_{1T}^2D(k_2)}+\frac{1}{k_{2T}^2D(k_1)}\right)+\frac{1}{\mathcal{O}M}\left(\frac{k_1^{-2}}{k_{1T}^2D(k_1)}+\frac{k_2^{-2}}{k_{2T}^2D(k_2)}\right)\right.\\ &\quad\left.+\frac{1}{k_{1T}^2k_{2T}^2D(k_1)D(k_2)}\right]\times\int d^2\mathbf{r}_Td^2\mathbf{b}_Te^{i(\mathbf{q}_T+\mathbf{k}_{1T}+\mathbf{k}_{2T})\cdot\mathbf{r}_T}N_F(\mathbf{b}_T,\mathbf{r}_T,x_g).\end{aligned} \tag{28}$$

The production at the partonic level is related to the one in proton-nucleus collisions by convoluting Eq. (28) with the quark and antiquark distribution functions of a proton and the quark-hadron fragmentation function

$$\frac{d\sigma^{qA\to h(q')\gamma(k_1)\gamma(k_2)X}}{d^2\mathbf{k}_{1T}d\eta_{\gamma_1}d^2\mathbf{k}_{2T}d\eta_{\gamma_3}d^2\mathbf{q}'_T d\eta_h}=\int_{z_h^{\min}}^1\frac{dz_h}{z_h^2}\int dx_q f(x_q,\mu_I^2)\frac{d\sigma^{q(p)\to q(q)\gamma(k_1)\gamma(k_2)X}}{d^2\mathbf{k}_{1T}d\eta_{\gamma_1}d^2\mathbf{k}_{2T}d\eta_{\gamma_2}d^2\mathbf{q}_T d\eta_h}D_{h/q}(z_h,\mu_F^2). \tag{29}$$

The light-cone momentum fractions x_q, x_g, z_h are again related to the transverse momenta and rapidities of the produced hadron and prompt diphoton via (see the Appendix for the derivation)

$$\begin{aligned}
x_q &= x_{\bar q}=\frac{1}{\sqrt{s}}\left(k_{1T}e^{\eta_{\gamma_1}}+k_{2T}e^{\eta_{\gamma_2}}+\frac{q'_T}{z_h}e^{\eta_h}\right),\\
x_g &= \frac{1}{\sqrt{s}}\left(k_{1T}e^{-\eta_{\gamma_1}}+k_{2T}e^{-\eta_{\gamma_2}}+\frac{q'_T}{z_h}e^{-\eta_h}\right),\\
z_h &= q'_T/q_T \quad \text{with} \quad z_h^{\min}=\frac{q'_T}{\sqrt{s}}\left(\frac{e^{\eta_h}}{1-\frac{k_{1T}}{\sqrt{s}}e^{\eta_{\gamma_1}}-\frac{k_{2T}}{\sqrt{s}}e^{\eta_{\gamma_2}}}\right).
\end{aligned} \tag{30}$$

One can obtain the inclusive diphoton cross section from the semi-inclusive diphoton + jet cross section given in Eq. (24) by integrating over the outgoing jet momentum. To simplify the algebra, we introduce photon fragmentation parameters z_1 and z_2. The parameters z_1 and z_2 are the fraction of energy of parton carried away by produced photons with momenta k_1 and k_2, respectively,

$$z_1=\frac{k_1^-}{p^-},\qquad z_2=\frac{k_2^-}{p^- - k_1^-}. \tag{31}$$

In the soft-photon limit, we have $z_1\approx\frac{k_1^-}{q^-}$ and $z_2\approx\frac{k_2^-}{q^-}$. Therefore, Eqs. (24) and (28) yield

$$\begin{aligned}
\frac{d\sigma^{qA\to\gamma(k_1)\gamma(k_2)X}}{d^2\mathbf{k}_{1T}d\eta_{\gamma_1}d^2\mathbf{k}_{2T}d\eta_{\gamma_2}}=&\frac{2\alpha_{em}^2e_q^4}{(2\pi)^6}z_1^2z_2^2\int d^2\mathbf{q}_T q_T^4\left[\frac{k_1^-k_2^-}{\mathcal{OM}}\left(\frac{1}{k_{1T}^2\mathcal{D}(k_2)}+\frac{1}{k_{2T}^2\mathcal{D}(k_1)}\right)+\frac{1}{\mathcal{OM}}\left(\frac{k_1^{-2}}{k_{1T}^2\mathcal{D}(k_1)}+\frac{k_2^{-2}}{k_{2T}^2\mathcal{D}(k_2)}\right)\right.\\
&\left.+\frac{1}{k_{1T}^2k_{2T}^2\mathcal{D}(k_1)\mathcal{D}(k_2)}\right]\int d^2\mathbf{r}_T d^2\mathbf{b}_T e^{i(\mathbf{q}_T+\mathbf{k}_{1T}+\mathbf{k}_{2T})\cdot\mathbf{r}_T}N_F(\mathbf{b}_T,\mathbf{r}_T,x_g),
\end{aligned} \tag{32}$$

with $\mathcal{O}$ defined in Eq. (26) and

$$\begin{aligned}
\mathcal{D}(k_i)&=(z_i\mathbf{q}_T-\mathbf{k}_{iT})^2 \quad \text{with} \quad i=1,2,\\
\mathcal{M}&=k_2^-\mathcal{D}(k_1)+k_1^-\mathcal{D}(k_2).
\end{aligned} \tag{33}$$

The relations between the light-cone variables x_g, z_1, z_2 and final-state momenta for inclusive diphoton production are given below (for the derivation, see the Appendix):

$$\begin{aligned}
x_g(q_T;k_{1T},\eta_{\gamma_1};k_{2T},\eta_{\gamma_2})&=\frac{1}{x_q s}\left[\frac{k_{1T}^2}{z_1}+\frac{k_{2T}^2}{z_2(1-z_1)}+\frac{q_T^2}{1-z_1-z_2+z_1z_2}\right],\\
z_1&=\frac{k_{1T}}{x_q\sqrt{s}}e^{\eta_{\gamma_1}},\\
z_2&=\frac{k_{2T}}{x_q(1-z_1)\sqrt{s}}e^{\eta_{\gamma_2}}.
\end{aligned} \tag{34}$$

Similar to Eqs. (20), (22), one can treat the collinear divergence in the cross section Eq. (32) by introducing a hard cutoff and separating the collinear singular part into the photon fragmentation contribution. The structure of the collinear singularity in different terms in Eq. (32) is very similar, except the last term which can be also rewritten in terms of two separated similar singular terms as long as $\frac{\mathbf{k}_{1T}}{z_1}\neq\frac{\mathbf{k}_{2T}}{z_2}$, using the identity

$$\frac{1}{\mathcal{D}(k_1)\mathcal{D}(k_2)}=\left(\frac{1}{\mathcal{D}(k_1)}+\frac{1}{\mathcal{D}(k_2)}\right)\frac{1}{\mathcal{D}(k_1)+\mathcal{D}(k_2)}. \tag{35}$$

It is convenient to perform some variable changes in Eq. (32). In the terms containing the factor $1/\mathcal{D}(k_1)$ and $1/\mathcal{D}(k_2)$, we change the variable q_T to $\mathbf{q}_T\to\mathbf{q}_T+\frac{\mathbf{k}_{1T}}{z_1}$ and $\mathbf{q}_T\to\mathbf{q}_T+\frac{\mathbf{k}_{2T}}{z_2}$, respectively. The infrared divergent part of the integral is then extracted in the same fashion as for the single inclusive photon production in Eq. (22). After some tedious but straightforward algebra, one can write the diphoton cross section in terms of fragmentation and direct parts,

$$\frac{d\sigma^{qA\to\gamma(k_1)\gamma(k_2)X}}{d^2\mathbf{k}_{1T}d\eta_{\gamma_1}d^2\mathbf{k}_{2T}d\eta_{\gamma_2}}=\frac{d\sigma^{\text{Direct}}}{d^2\mathbf{k}_{1T}d\eta_{\gamma_1}d^2\mathbf{k}_{2T}d\eta_{\gamma_2}}+\frac{d\sigma^{\text{Fragmentation}}}{d^2\mathbf{k}_{1T}d\eta_{\gamma_1}d^2\mathbf{k}_{2T}d\eta_{\gamma_2}}. \tag{36}$$

The direct diphoton contribution is given by

$$\begin{aligned}\frac{d\sigma^{\text{Direct}}}{d^2\mathbf{k}_{1T}d\eta_{\gamma_1}d^2\mathbf{k}_{2T}d\eta_{\gamma_2}}=&\frac{2\alpha_{em}^2e_q^4}{(2\pi)^6}\int_{q_T^2>\mu_F^2}d^2\mathbf{q}_T\frac{|\mathbf{q}_T+\mathbf{k}_{1T}/z_1|^4}{q_T^2}N_F(|\mathbf{q}_T+\mathbf{k}_{1T}(1+1/z_1)+\mathbf{k}_{2T}|,x_g(|\mathbf{q}_T+\mathbf{k}_{1T}/z_1|))\\&\times z_2^2\left[\frac{1}{k_{1T}^2k_{2T}^2(q_T^2z_1^2+z_2^2|\mathbf{q}_T+\mathbf{k}_{1T}/z_1-\mathbf{k}_{2T}/z_2|^2)}\right.\\&\left.+\left(\frac{k_1^-k_2^-}{\mathcal{O}k_{2T}^2}+\frac{k_1^{-2}}{\mathcal{O}k_{1T}^2}\right)\frac{1}{k_2^-q_T^2z_1^2+k_1^-z_2^2|\mathbf{q}_T+\mathbf{k}_{1T}/z_1-\mathbf{k}_{2T}/z_2|^2}\right]+(k_1\leftrightarrow k_2,z_1\leftrightarrow z_2).\end{aligned} \tag{37}$$

The fragmentation contribution can be written in terms of a single and double photon fragmentation functions,

$$\begin{aligned}\left.\frac{d\sigma^{\text{Fragmentation}}}{d^2\mathbf{k}_{1T}d\eta_{\gamma_1}d^2\mathbf{k}_{2T}d\eta_{\gamma_2}}\right|_{\frac{\mathbf{k}_{1T}}{z_1}\neq\frac{\mathbf{k}_{2T}}{z_2}}=&\frac{\alpha_{em}e_q^2}{2(2\pi)^4}\frac{k_{1T}^2z_2^2}{|\mathbf{k}_{1T}z_2-\mathbf{k}_{2T}z_1|^2}\left[\frac{1}{k_{2T}^2}+\frac{k_{1T}^2k_2^-}{k_{2T}^2\mathcal{O}}+\frac{k_1^-}{\mathcal{O}}\right]\frac{1}{z_1}D_{\gamma/h}(z_1,\mu_F^2)\\&\times N_F(|\mathbf{k}_{1T}(1+1/z_1)+\mathbf{k}_{2T}|,x_g(k_{1T}/z_1))+(k_1\leftrightarrow k_2,z_1\leftrightarrow z_2),\\\left.\frac{d\sigma^{\text{Fragmentation}}}{d^2\mathbf{k}_{1T}d\eta_{\gamma_1}d^2\mathbf{k}_{2T}d\eta_{\gamma_2}}\right|_{\frac{\mathbf{k}_{1T}}{z_1}=\frac{\mathbf{k}_{2T}}{z_2}}=&\frac{\alpha_{em}e_q^2}{2(2\pi)^4}\left[\frac{1}{2}+(k_1^-k_2^-k_{1T}^2+k_1^{-2}k_{2T}^2)\frac{z_2^2}{\mathcal{O}(k_2^-z_1^2+k_1^-z_2^2)}\right]\frac{1}{z_1z_2}D_{\gamma_1\gamma_2/h}(z_1,z_2,\mu_F^2)\\&\times N_F(|\mathbf{k}_{1T}(1+1/z_1)+\mathbf{k}_{2T}|,x_g(k_{1T}/z_1))+(k_1\leftrightarrow k_2,z_1\leftrightarrow z_2).\end{aligned} \tag{38}$$

The single-photon fragmentation function $D_{\gamma/h}$ was defined in Eq. (23), and the diphoton fragmentation function in the soft limit in the leading-log approximation is

$$D_{\gamma_1\gamma_2/h}(z_1,z_2,\mu_F^2)=\frac{\alpha_{em}e_q^2}{\pi}\frac{1}{z_1z_2}\left(\frac{1}{\Lambda_{QCD}^2}-\frac{1}{\mu_F^2}\right). \tag{39}$$

In Eqs. (37) and (38), we used a short-hand notation for the light-cone variable $x_g(q_T)\equiv x_g(q_T;k_{1T},\eta_{\gamma_1};k_{2T},\eta_{\gamma_2})$, where x_g was defined in Eq. (34). Therefore, one should bear in mind that in different terms in direct and fragmentation parts, the arguments of the dipole-target scattering amplitude $N_F(k_T,x_g)$ (the transverse momenta k_T and gluon light-cone variable x_g) are different.

Note that, as long as $\frac{\mathbf{k}_{1T}}{z_1}\neq\frac{\mathbf{k}_{2T}}{z_2}$, the two collinear singularities of the integrand in Eq. (32) do not coincide, and therefore the diphoton fragmentation contribution in Eq. (38) can be written in terms of two single-photon fragmentation contributions. When $\frac{\mathbf{k}_{1T}}{z_1}\approx\frac{\mathbf{k}_{2T}}{z_2}$, the collinear singularity in Eq. (32) is stronger than the case of the single-photon production in Eqs. (22) and (23).

Both the semi-inclusive diphoton + jet and inclusive diphoton production cross section (both direct and fragmentation parts) depend on the dipole-target amplitude and therefore in principle probe the small-x dynamics. In contrast to the dihadron production at leading-log which involves a higher number of Wilson lines, the diphoton production depends only on the dipole amplitude. Note that the light-cone variables x_g and x_q that enter the diphoton + jet and diphoton production cross sections are different; see Eqs. (30) and (34). Therefore, the two cross sections in principle are sensitive to different kinematical regions of the dipole amplitude.

The production in proton-nucleus collisions is related to the above partonic cross section via

$$\frac{d\sigma^{pA\to\gamma(k_1)\gamma(k_2)X}}{d^2\mathbf{k}_{1T}d\eta_{\gamma_1}d^2\mathbf{k}_{2T}d\eta_{\gamma_2}}=\int_{x_q^{\min}}^1 dx_q[f_q(x_q,\mu_I^2)+f_{\bar{q}}(x_{\bar{q}},\mu_I^2)]\times\frac{d\sigma^{qA\to\gamma(k_1)\gamma(k_2)X}}{d^2\mathbf{k}_{1T}d\eta_{\gamma_1}d^2\mathbf{k}_{2T}d\eta_{\gamma_2}},\tag{40}$$

where the parameter x_q is the ratio of the incoming quark to the projectile nucleon energy and the lower limit of integral $x_q^{\min}$ is defined by

$$x_q^{\min}=Max\left(\frac{k_{1T}e^{\eta_{\gamma_1}}}{\sqrt{s}},\frac{k_{2T}e^{\eta_{\gamma_2}}}{\sqrt{s}-k_{1T}e^{\eta_{\gamma_1}}}\right).\tag{41}$$

Before proceeding with numerical computation, a comment here is in order. In the soft limit, we assumed that for large s the "−" component of the incoming projectile momentum is approximately unchanged by the interaction, and the transverse momenta of the emitted photons are small, $k_{1T},k_{2T}\lesssim q_T$ with $\mathbf{q}^2/s\ll 1$. This approximation is not appropriate for $q_T=0$. Since the produced quark momentum is integrated over to obtain the inclusive diphoton cross section, it is essential to check that the contribution of this kinematic region is not important. Under the kinematic condition that $p^-\approx q^-$ and $q_T=0$, the trace in Eq. (11) can be analytically calculated to give

$$\langle \mathrm{tr}(S^\dagger S)\rangle_{\mathrm{spin}}=\frac{8(k_1.k_2)^2(k_1^++k_2^+)^2[(k_1^+-k_2^+)^2p^{-2}-(k_1.k_2)^2]}{(k_1^+k_2^+)^2[(k_1^++k_2^+)^2p^{-2}-(k_1.k_2)^2]^2},\tag{42}$$

where for $\mathbf{q}_T=0$ one has $k_1^++k_2^+\approx x_g\sqrt{s/2}$ and $q^-=p^-\approx x_q\sqrt{s/2}$. After straightforward algebra, one can show that z_1 and z_2 dependence of the two expressions, Eqs. (42) and (25) is similar, and for $z_1,z_2\to 0$ the above expression approaches zero. Moreover, for the inclusive diphoton production, the expression Eq. (42) enters the cross section multiplied by a factor that vanishes at small q_T. Therefore, the contribution of this kinematical region to the inclusive diphoton cross section is indeed negligible.

III. NUMERICAL RESULTS AND DISCUSSION

The main ingredient in the calculation of the cross section of semi-inclusive diphoton + jet production in Eq. (28), inclusive direct, and fragmentation diphoton production [Eqs. (37) and (38)] is the two-dimensional Fourier transform of the universal dipole-target forward scattering amplitude N_F. It incorporates small-x dynamics and can be calculated by solving the nonlinear JIMWLK equations [3]. In the large N_c limit, the coupled JIMWLK equations are simplified to the Balitsky–Kovchegov (BK) equation [4], a closed-form equation for the rapidity evolution of the dipole amplitude which is presently known to next-to-leading accuracy [5,6]. The running-coupling improved BK equation (rcBK) has the same generic formal form as the leading-log BK evolution equation,

$$\frac{\partial N_F(r,x)}{\partial\ln(x_0/x)}=\int d^2\vec{r}_1K^{\mathrm{run}}(\vec{r},\vec{r}_1,\vec{r}_2)[N_F(r_1,x)+N_F(r_2,x)-N_F(r,x)-N_F(r_1,x)N_F(r_2,x)],\tag{43}$$

where the modified evolution kernel K^{run} using Balitsky's prescription [49] for the running coupling is given by

$$K^{\mathrm{run}}(\vec{r},\vec{r}_1,\vec{r}_2)=\frac{N_c\alpha_s(r^2)}{2\pi^2}\left[\frac{1}{r_1^2}\left(\frac{\alpha_s(r_1^2)}{\alpha_s(r_2^2)}-1\right)+\frac{r^2}{r_1^2r_2^2}+\frac{1}{r_2^2}\left(\frac{\alpha_s(r_2^2)}{\alpha_s(r_1^2)}-1\right)\right],\tag{44}$$

with $\vec{r}_2\equiv\vec{r}-\vec{r}_1$ [49,50]. The only external input necessary for solving the rcBK nonlinear equation is the initial condition for the amplitude. We take it to have the following form, motivated by the McLerran–Venugopalan model [2]:

$$N(r,Y=0)=1-\exp\left[-\frac{(r^2Q_{0s}^2)^\gamma}{4}\ln\left(\frac{1}{\Lambda_{QCD}r}+e\right)\right].\tag{45}$$

The infrared scale is taken as $\Lambda_{QCD}=0.241$ GeV, and the onset of the small-x evolution is assumed to be at $x_0=0.01$ [7]. The free parameters in the rcBK equation are γ and the initial saturation scale Q_{0s} (as probed by quarks), with $s=p,A$ for the proton and nuclear target, respectively. The initial saturation scale of proton $Q_{0p}^2\simeq 0.168$ GeV^2 with the corresponding $\gamma\simeq 1.119$ was extracted from a global fit to proton structure functions in deep inelastic scattering (DIS) in the small-x region [7] and single inclusive hadron data in p + p collisions at RHIC and the LHC [14,17,21]. Note that the current HERA data alone are not enough to uniquely fix the values of Q_{0p} and γ [7]. For the nucleus case, the initial saturation scale of a nucleus $Q_{0A}^2\approx 5Q_{0p}^2$ should be considered as an impact-parameter averaged value, and it is extracted from the minimum-bias data in deuteron-gold collisions at RHIC and proton-lead collisions at the LHC [17].

Let us define the azimuthal correlation of the produced diphoton as [36,37]

$$C(\Delta\phi) = \frac{d\sigma^{pA\to\gamma(k_1)\gamma(k_2)X}}{d^2\mathbf{k}_{1T}d\eta_{\gamma_1}d^2\mathbf{k}_{2T}d\eta_{\gamma_2}}[\Delta\phi] \Big/ \frac{d\sigma^{pA\to\gamma(k_1)\gamma(k_2)X}}{d^2\mathbf{k}_{1T}d\eta_{\gamma_1}d^2\mathbf{k}_{2T}d\eta_{\gamma_2}}[\Delta\phi = \Delta\phi_c], \tag{46}$$

where $\Delta\phi$ is the azimuthal angle between the two produced photons in the plane transverse to the collision axis. The azimuthal correlation C is proportional to the probability of inclusive diphoton pair production in a given kinematics and angle $\Delta\phi$ between the photons in the pair, normalized to the fixed reference angle $\Delta\phi_c$. Since we are mostly interested in studying correlations at $\Delta\phi \approx \pi$, we fix the reference angle $\Delta\phi_c = \pi/2$ throughout this paper.

One can equally well take the normalization in Eq. (46) as the differential cross section integrated over the angle $\Delta\phi$. We expect that some of the theoretical uncertainties, such as sensitivity to possible K factors, which effectively incorporates the missing higher order corrections, drop out in the correlation defined in Eq. (46). One should bear in mind that the correlation defined in Eq. (46) may be more challenging to measure compared to the so-called coincidence probability [37,51,52] due to possible underlying event dependence; however, since it is free from extra integrals over transverse momenta, it should exhibit the underlying dynamics of the correlation in a cleaner way. In a sense, the correlation defined in Eq. (46) is a snapshot of the integrand in the coincidence probability.

Note that the hard scale μ_I in the parton distribution in Eq. (40) can be in principle different from the photon fragmentation scale μ_F introduced in Eqs. (37) and (38). Following the conventional pQCD approach, we take the hard scale μ_I to be equal to the fragmentation scale μ_F, namely, $\mu = \mu_F = \mu_I$. We will later quantify uncertainties associated with the freedom to choose a different scale μ. For the patron distributions, we will use the next-to-leading-order (NLO) Martin-Stirling-Thorne-Watt (MSTW) PDFs [53]. For numerical computation, we focus here at low transverse momenta of the produced photon pair at the LHC at forward rapidities, consistent with the soft approximation employed for obtaining the cross section. Note that this kinematics is mostly relevant for probing saturation effects.

In the standard perturbative calculations, the leading contribution to the diphoton production comes from the annihilation diagram. This process produces back-to-back photon pairs and thus leads to a strong peak in the correlation at $\Delta\phi = \pi$. This contribution is absent in the CGC approach, since the dense target wave function is dominated by gluons. In the CGC framework, the annihilation contribution only appears in the next order in α_s. Nevertheless, we expect the fragmentation diphoton to have a non-negligible correlation peaked at $\Delta\phi = \pi$. The reason is that the photon-quark Fock component of the incoming quark has zero transverse momentum in the collinear factorization approach. Therefore, if momentum transfer from the target is small enough, the photon collinear to the outgoing quark and the photon emerging from the initial photon-quark state will have opposite transverse momenta, leading to back-to-back correlation.

The direct diphoton part, on the other hand, is restricted to kinematics where the transverse momentum of the outgoing quark jet is relatively large $q_T > \mu_F$. One therefore does not expect significant back-to-back correlation in the direct photon contribution and also expects that the correlations in the direct part should be more sensitive to the fragmentation scale. Reducing the scale μ should enhance the back-to-back correlations for the direct diphoton.[2]

Indeed, our numerical results shown in Fig. 2 follow these expectations. Note that, because of the convolution with fragmentation and parton distribution functions, the partonic level correlation gets somewhat smeared out. In Fig. 2, we show that the correlations at $\Delta\phi = \pi$ in the direct diphoton contribution are indeed much smaller than in the fragmentation one. In Fig. 2, we also show the effects of different fragmentation/factorization scales. We present the correlations in different components of diphoton production calculated with two different scales μ (left panel) and $\mu/2$ (right panel).

The fragmentation contribution is less sensitive to the choice of fragmentation/factorization scale while the correlations in the direct diphoton are affected by this uncertainty. This is easy to understand since the fragmentation/factorization scale that appears in the FF and the PDF of fragmentation cross section in Eq. (38) mainly cancels between the numerator and the denominator in the correlation defined in Eq. (46). This does not happen in the direct part since the fragmentation scale appears as the lower limit of the integral in the cross section, Eq. (37).

In Fig. 2, we also compare the correlations of direct, fragmentation, and prompt (fragmentation + direct) diphoton production at fixed kinematics at the LHC in proton-nucleus collisions for two different fragmentation/factorization scales. One notes that the back-to-back correlation is larger in the fragmentation part, while the total (and near-side) direct diphoton cross section is larger than the fragmentation one. As a result, the total prompt diphoton signal (the sum of direct and fragmentation parts) exhibits a reduced back-to-back correlation defined via Eq. (46). However, with the isolation cut technique [41] (see also Ref. [54]), one can in principle isolate the

[2]Note that this is one of the main differences between diphoton and dihadron correlations. In the later case, the dihadron can be produced from splitting a single gluon, and the back-to-back production is in principle kinematically allowed.

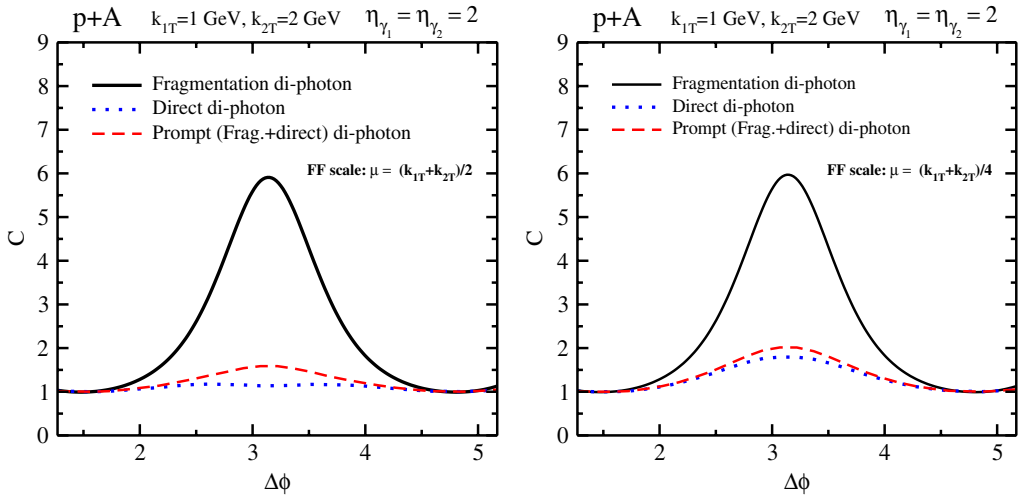

FIG. 2 (color online). Correlations of fragmentation, direct, and prompt diphoton production for two different fragmentation/factorization scales μ (left panel) and $\mu/2$ (right panel), where we defined $\mu = \mu_F = \mu_I = (k_{1T} + k_{2T})/2$. All curves are results obtained at a fixed pseudorapidity $\eta_{\gamma_1} = \eta_{\gamma_2} = 2$ and fixed transverse momenta $k_{1T} = 1$ GeV, and $k_{2T} = 2$ GeV in minimum-bias proton-lead (p + A) collisions at the LHC $\sqrt{s} = 8.8$ TeV.

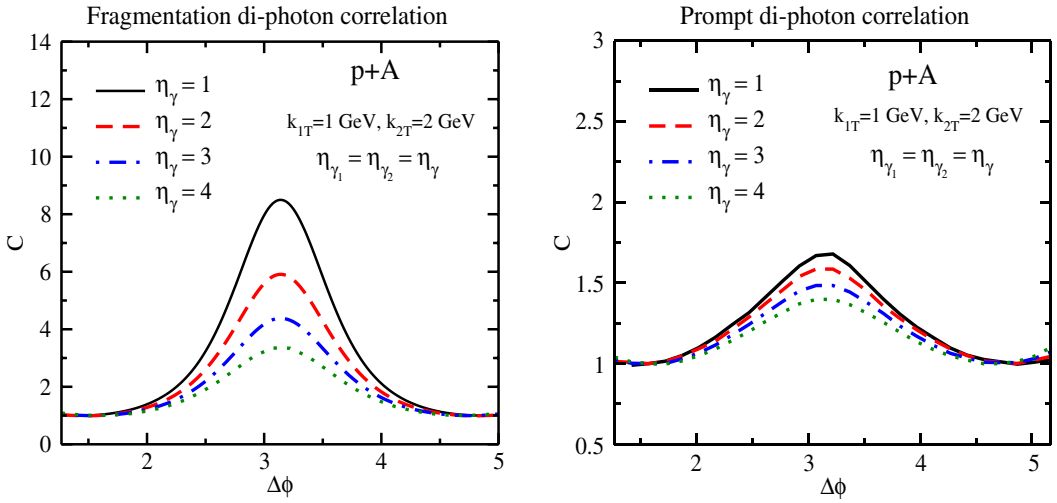

FIG. 3 (color online). Fragmentation (left panel) and prompt (right panel) diphoton correlations at different pseudorapidities of the produced diphoton $\eta = \eta_{\gamma_1} = \eta_{\gamma_2}$ in minimum-bias proton-lead collisions. In both panels, the curves are the results obtained from the rcBK evolution equation with transverse momenta of the diphoton, fixed at $k_{1T} = 1$ GeV, and $k_{2T} = 2$ GeV at LHC energy $\sqrt{s} = 8.8$ TeV. In both panels, the factorization and fragmentation scales are taken to be equal to $\mu_F = \mu_I = (k_{1T} + k_{2T})/2$.

fragmentation diphoton contribution and study this correlation separately.[3] Note also that, by default, the back-to-back correlation is significantly larger in the two single-photon fragmentation than double-photon fragmentation parts; see Eq. (38).

In Fig. 3 we show the rapidity dependence of the fragmentation and prompt (direct + fragmentation) diphoton correlation C defined in Eq. (46) at fixed transverse momenta of the produced diphoton in minimum-bias proton-nucleus collisions at the LHC energy $\sqrt{s} = 8.8$ TeV. The back-to-back correlations are systematically suppressed at forward rapidities (larger η_{γ_1} and η_{γ_2}) in both fragmentation and prompt (and direct) diphoton production.

Given that the correlation in the direct diphoton production is small (see Figs. 2 and 3), in the following we only show the correlation calculated from the fragmentation diphoton part. The general features of the (de)correlations discussed below persist for the prompt diphoton

[3]This would be the opposite of what one may do in order to study the direct diphoton (or photon) production by imposing isolation cut to discard the fragmentation contribution. An incorporation of the isolation cut criterion in our framework is beyond the scope of the current paper.

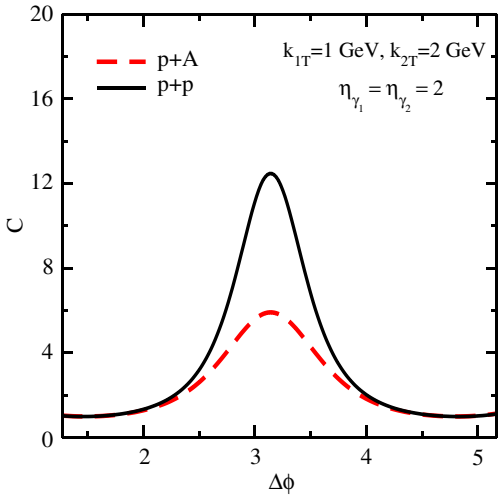

FIG. 4 (color online). Comparison of fragmentation diphoton correlations in minimum-bias proton-proton and proton-lead collisions at a fixed pseudorapidity $\eta_{\gamma_1} = \eta_{\gamma_2} = 2$ with $k_{1T} = 1$ GeV and $k_{2T} = 2$ GeV at the LHC energy $\sqrt{s} = 8.8$ TeV.

production, albeit the magnitude of the correlation is uniformly smaller. We also fix the factorization/fragmentation scale to $\mu = (k_{1T} + k_{2T})/2$, as the variation of the scale does not greatly affect the correlations in the fragmentation part; see Fig. 2.

In Fig. 4, we compare the diphoton correlations in minimum-bias $p + p$ and $p + A$ collisions at forward rapidity $\eta_{\gamma_1} = \eta_{\gamma_2} = 2$ for fixed transverse momenta of the pair at $k_{1T} = 1$ GeV and $k_{2T} = 2$ GeV. The back-to-back correlations in $p + A$ collisions are clearly suppressed compared to $p + p$ collisions.

In Fig. 5, right panel, we show the effect of variation of transverse momenta of the produced photons at fixed rapidity in $p + A$ collisions at the LHC. Lowering the transverse momenta leads to suppression of the away-side diphoton correlation.

Note that all the features seen in Figs. 3, 4, and 5can be understood in the saturation picture. By increasing density or rapidity/energy or decreasing transverse momenta, the typical x_g which enters in the dipole-target scattering amplitude becomes smaller, and consequently the typical saturation scale of the system becomes larger. In this case, the intrinsic back-to-back correlation is smeared due to momentum exchange with the target at the saturation scale. This increased decorrelation with increasing saturation scale appears to be a universal feature of diphoton production, irrespective of the mechanism by which the saturation scale is increased.

IV. CONCLUSION

In this paper we investigated semi-inclusive diphoton + jet and inclusive diphoton production at leading-log approximation in high-energy proton-nucleus collisions using the color-glass condensate formalism. We obtained the inclusive prompt diphoton cross section in terms of fragmentation and direct diphoton contributions while the fragmentation part is given in terms of single-photon and double-photon fragmentation functions.

We have also studied the diphoton azimuthal angular correlations in $p + p$ and $p + A$ collisions at the LHC kinematics. It is generally seen that at low transverse momenta of the produced diphoton back-to-back correlations of fragmentation, direct, and prompt diphoton production are all sensitive to saturation physics, although this sensitivity is significantly stronger in two single-photon fragmentation parts. It was shown that the away-side peak in diphoton angular correlation is reduced by lowering the diphoton transverse momenta. At a fixed transverse

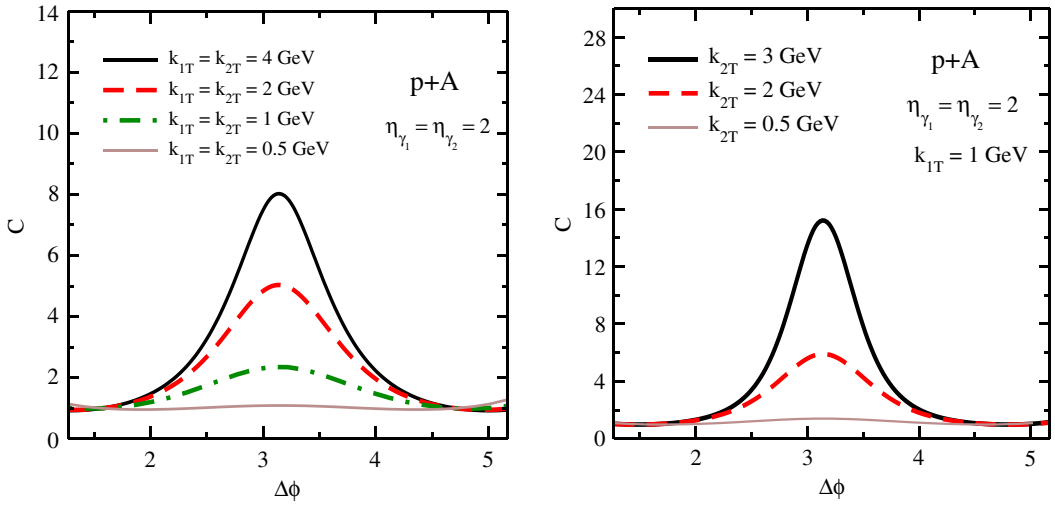

FIG. 5 (color online). Diphoton (fragmentation) correlations at different transverse momenta of the produced photon pair k_{1T} and k_{2T} in minimum-bias proton-lead collisions. In both panels, the curves are the results obtained at a fixed pseudorapidity $\eta_{\gamma_1} = \eta_{\gamma_2} = 2$ in proton-lead collisions at the LHC $\sqrt{s} = 8.8$ TeV.

momenta, the suppression of the away-side correlations gets stronger as one goes to larger rapidities (or higher energies) or a denser system. The main features of away-side decorrelation of diphoton production seem to be universally similar to that in dihadron [35] and photon-hadron [36,37] productions in high-energy p + A collisions. In all cases, the away-side correlations of the produced diparticle get suppressed in the presence of a large saturation scale irrespective of mechanism by which the particles are produced and the saturation scale is enhanced. We recall that diphoton production is a theoretically cleaner probe of initial-state effects and small-x dynamics compared to dihadron production, mainly due to the fact that the diphoton production is free from hadronization corrections, which theoretically are not too well understood. Moreover, since the virtual photons do not interact with the gluons inside target, final-state effects are absent in the diphoton production.

ACKNOWLEDGMENTS

The authors would like to thank Jamal Jalilian-Marian for fruitful discussions at early stage of this work. A. K. thanks Physics Department of Universidad Técnica Federico Santa María for hospitality. The work of A. H. R. is supported in part by Fondecyt Grant No. 1110781. The work of A. K. is supported by DOE Grant No. DE-FG02-13ER41989.

APPENDIX

The purpose of this appendix is to define the kinematics and derive the needed relations between various light-cone energy fractions which appear in the production cross sections used. This is slightly different from the standard relations used in production cross sections based on collinear factorization theorems of perturbative QCD (pQCD). We first consider scattering of a quark on the target where a photon and a quark are produced, depicted in Fig. 1,

$$q(p)+A(p_A)\to\gamma(k_1)+\gamma(k_2)+\mathrm{jet}(q)+X, \tag{A1}$$

where A is a label for the multigluon state, described by a classical field representing a proton or nucleus target. In the standard pQCD (leading twist) kinematics, only one parton from the target interacts. This is not the case here since the target is described by a classical gluon field representing a multigluon state with intrinsic momentum rather than an individual gluon with a well-defined energy fraction x_g and zero transverse momentum. Nevertheless, since most of the gluons in the target wave function have momentum of order Q_s, one can think of the state describing the target as being labeled by a (4-)momentum p_A. In this sense, the gluons in the target collectively carry fraction x_g of the target energy and have intrinsic transverse momentum denoted by $\mathbf{p}_A$. This also means that there is no integration over x_g in our case, unlike the collinearly factorized cross sections in pQCD (this basically corresponds to setting x_g equal to the lower limit of x_g integration in pQCD cross sections). We thus have

$$\begin{aligned}
p^\mu &= (p^-=x_q\sqrt{s/2},\, p^+=0,\, \mathbf{p}_T=0),\\
P^\mu &= (P^-=\sqrt{s/2},\, P^+=0,\, \mathbf{P}_T=0),\\
p_A^\mu &= (p_A^-=0,\, p_A^+=x_g\sqrt{s/2},\, \mathbf{p}_{AT}),\\
P_A^\mu &= (P_A^-=0,\, P_A^+=\sqrt{s/2},\, \mathbf{P}_{AT}=0),\\
q^\mu &= (q^-,\, q^+=q_T^2/2q^-,\, \mathbf{q}_T),\\
k_1^\mu &= (k_1^-=z_1p^-=z_1x_q\sqrt{s/2},\, k_1^+=k_{1T}^2/2k_1^-,\, \mathbf{k}_{1T}),\\
k_2^\mu &= (k_2^-=z_2(p^--k_1^-)=x_qz_2(1-z_1)\sqrt{s/2},\\
&\quad k_2^+=k_{2T}^2/2k_2^-,\, \mathbf{k}_{2T}),
\end{aligned} \tag{A2}$$

where P^μ, P_A^μ, q^μ are the momenta of the incoming projectile, target, and the produced jet, respectively. (Pseudo)rapidities of the produced diphoton are related to their energies via

$$k_1^-=\frac{k_{1T}}{\sqrt{2}}e^{\eta_{\gamma_1}},\qquad k_2^-=\frac{k_{2T}}{\sqrt{2}}e^{\eta_{\gamma_2}},\qquad q^-=\frac{q_T}{\sqrt{2}}e^{\eta_h}. \tag{A3}$$

Imposing energy-momentum conservation at the partonic level via $\delta^4(p+p_A-q-k_1-k_2)$ and using Eq. (A2) leads to

$$p^-=k_1^-+k_2^-+q^-, \tag{A4}$$

$$p_A^+=k_1^++k_2^++q^+, \tag{A5}$$

$$\mathbf{p}_{AT}=\mathbf{k}_{1T}+\mathbf{k}_{2T}+\mathbf{q}_T. \tag{A6}$$

Plugging the definitions given in Eq. (A3) into the above relations and using Eq. (A2) (and the on mass-shell condition), one can immediately obtain the energy fractions x_q, x_g in the case of the diphoton + jet production,

$$\begin{aligned}
x_q &= x_{\bar{q}}=\frac{1}{\sqrt{s}}(k_{1T}e^{\eta_{\gamma_1}}+k_{2T}e^{\eta_{\gamma_2}}+q_Te^{\eta_h}),\\
x_g &= \frac{1}{\sqrt{s}}(k_{1T}e^{-\eta_{\gamma_1}}+k_{2T}e^{-\eta_{\gamma_2}}+q_Te^{-\eta_h}),
\end{aligned} \tag{A7}$$

where the first and second equations were directly derived from Eqs. (A4) and (A5), respectively. Note that the light-cone momentum fraction x_g appears in the dipole forward scattering amplitude $N_F(b_t, r_t, x_g)$, whereas x_q is the fraction of the projectile proton carried by the incident quark; see Eq. (A2). One can relate the transverse momentum of the fragmented hadron q_T' to the outgoing quark q_T via $z_h=q_T'/q_T$. Now using Eq. (A4) the minimum value of z_h is obtained for the maximum value of $x_q=1$. Therefore, we obtain

$$z_h^{\min} = \frac{q'^-}{\sqrt{s/2} - k_1^- - k_2^-}. \tag{A8}$$

For obtaining the diphoton production, one integrates over the outgoing quark transverse momentum and rapidity of diphoton + jet cross section. The integral over rapidity of the outgoing jet or q^- can be done analytically. Therefore, some extra care is in order here. Let us first introduce the parameters z_1 and z_2 as the fraction of energy of parton carried away by two produced photons defined by

$$z_1 \equiv \frac{k_1^-}{p^-} = \frac{k_{1T}}{x_q\sqrt{s}} e^{\eta_{\gamma_1}},$$
$$z_2 \equiv \frac{k_2^-}{p^- - k_1^-} = \frac{k_{2T}}{x_q(1-z_1)\sqrt{s}} e^{\eta_{\gamma_2}}. \tag{A9}$$

Plugging the above relations into Eqs. (A4) and (A5) and using Eq. (A2), one can derive the following expressions for the energy fractions x_q, x_g:

$$x_q = x_{\bar{q}} = \frac{q^-}{\sqrt{s/2}(1 - z_1 - z_2 + z_2 z_1)}, \tag{A10}$$

$$x_g = \frac{1}{x_q s}\left[\frac{k_{1T}^2}{z_1} + \frac{k_{2T}^2}{z_2(1-z_1)} + \frac{q_T^2}{1 - z_1 - z_2 + z_1 z_2}\right]. \tag{A11}$$

To derive an expression for the lower limit of z_1 and z_2 (in integration), we note that $0 \le x_q \le 1$. Using the relations in Eq. (A9), we obtain

$$z_1^{\min} = \frac{k_{1T} e^{\eta_{\gamma_1}}}{\sqrt{s}},$$
$$z_2^{\min} = \frac{k_{2T} e^{\eta_{\gamma_2}}}{\sqrt{s}(1 - z_1^{\min})} = \frac{k_{2T} e^{\eta_{\gamma_2}}}{\sqrt{s} - k_{1T} e^{\eta_{\gamma_1}}}. \tag{A12}$$

Equally, we can immediately obtain the lowest value of x_q denoted by $x_q^{\min}$ from Eqs. (A9) and (A12) by imposing the condition that $0 < z_1, z_2 < 1$,

$$x_q^{\min} = \mathrm{Max}\left(\frac{k_{1T} e^{\eta_{\gamma_1}}}{\sqrt{s}}, \frac{k_{2T} e^{\eta_{\gamma_2}}}{\sqrt{s} - k_{1T} e^{\eta_{\gamma_1}}}\right). \tag{A13}$$

[1] L. V. Gribov, E. M. Levin, and M. G. Ryskin, Phys. Rep. **100**, 1 (1983); A. H. Mueller and J-W. Qiu, Nucl. Phys. **268**, 427 (1986).
[2] L. D. McLerran and R. Venugopalan, Phys. Rev. D **49**, 2233 (1994); **49**, 3352 (1994); **50**, 2225 (1994).
[3] J. Jalilian-Marian, A. Kovner, A. Leonidov, and H. Weigert, Nucl. Phys. **B504**, 415 (1997); Phys. Rev. D **59**, 014014 (1998); E. Iancu, A. Leonidov, and L. D. McLerran, Nucl. Phys. **A692**, 583 (2001); E. Ferreiro, E. Iancu, A. Leonidov, and L. D. McLerran, Nucl. Phys. **A703**, 489 (2002).
[4] I. Balitsky, Nucl. Phys. **B463**, 99 (1996); Y. V. Kovchegov, Phys. Rev. D **60**, 034008 (1999); **61**, 074018 (2000).
[5] I. Balitsky and G. A. Chirilli, Phys. Rev. D **77**, 014019 (2008).
[6] A. Kovner, M. Lublinsky, and Y. Mulian, Phys. Rev. D **89**, 061704 (2014).
[7] J. L. Albacete, N. Armesto, J. G. Milhano, P. Quiroga Arias, and C. A. Salgado, Eur. Phys. J. C **71**, 1705 (2011).
[8] A. H. Rezaeian, M. Siddikov, M. Van de Klundert, and R. Venugopalan, Phys. Rev. D **87**, 034002 (2013).
[9] A. H. Rezaeian and I. Schmidt, Phys. Rev. D **88**, 074016 (2013).
[10] D. Kharzeev and M. Nardi, Phys. Lett. B **507**, 121 (2001); D. Kharzeev, E. Levin, and M. Nardi, Nucl. Phys. **A747**, 609 (2005).
[11] A. Dumitru, A. Hayashigaki, and J. Jalilian-Marian, Nucl. Phys. **A765**, 464 (2006); **A770**, 57 (2006).
[12] I. Arsene *et al.* (BRAHMS Collaboration), Nucl. Phys. **A757**, 1 (2005) and references therein.
[13] E. Levin and A. H. Rezaeian, Phys. Rev. D **82**, 014022 (2010).
[14] J. L. Albacete and A. Dumitru, arXiv:1011.5161.
[15] P. Tribedy and R. Venugopalan, Phys. Lett. B **710**, 125 (2012).
[16] J. L. Albacete, A. Dumitru, H. Fujii, and Y. Nara, Nucl. Phys. **A897**, 1 (2013).
[17] A. H. Rezaeian, Phys. Lett. B **718**, 1058 (2013).
[18] E. Levin and A. H. Rezaeian, Phys. Rev. D **82**, 054003 (2010); **83**, 114001 (2011); A. H. Rezaeian, Phys. Rev. D **85**, 014028 (2012).
[19] B. Schenke, P. Tribedy, and R. Venugopalan, Phys. Rev. Lett. **108**, 252301 (2012); , **86**, 034908 (2012); A. Bzdak, B. Schenke, P. Tribedy, and R. Venugopalan, Phys. Rev. C **87**, 064906 (2013).
[20] A. H. Rezaeian, Phys. Lett. B **727**, 218 (2013).
[21] J. Jalilian-Marian and A. H. Rezaeian, Phys. Rev. D **85**, 014017 (2012).
[22] L. McLerran, arXiv:hep-ph/0311028.
[23] F. Gelis, E. Iancu, J. Jalilian-Marian, and R. Venugopalan, Annu. Rev. Nucl. Part. Sci. **60**, 463 (2010).
[24] J. L. Albacete and C. Marquet, Prog. Part. Nucl. Phys. **76**, 1 (2014).
[25] J. L. Albacete *et al.*, Int. J. Mod. Phys. E **22**, 1330007 (2013).
[26] N. Armesto and A. H. Rezaeian, arXiv:1402.4831.

[27] A. Dumitru, F. Gelis, L. McLerran, and R. Venugopalan, Nucl. Phys. **A810**, 91 (2008); S. Gavin, L. McLerran, and G. Moschelli, Phys. Rev. C **79**, 051902 (2009); Y. V. Kovchegov, E. Levin, and L. D. McLerran, Phys. Rev. C **63**, 024903 (2001).

[28] A. Dumitru, K. Dusling, F. Gelis, J. Jalilian-Marian, T. Lappi, and Venugopalan, Phys. Lett. B **697**, 21 (2011); K. Dusling and R. Venugopalan, Phys. Rev. D **87**, 094034 (2013).

[29] A. Dumitru and J. Jalilian-Marian, Phys. Rev. D **81**, 094015 (2010).

[30] A. Kovner and M. Lublinsky, Phys. Rev. D **83**, 034017 (2011); **84**, 094011 (2011).

[31] E. Levin and A. H. Rezaeian, Phys. Rev. D **84**, 034031 (2011).

[32] E. Iancu and D. Triantafyllopoulos, J. High Energy Phys. 11 (2011) 105.

[33] Y. V. Kovchegov and D. E. Wertepny, arXiv:1310.6701.

[34] For a review, see A. Kovner, and M. Lublinsky, Int. J. Mod. Phys. E **22**, 1330001 (2013) and references therein.

[35] C. Marquet, Nucl. Phys. **A796**, 41 (2007); J. L. Albacete and C. Marquet, Phys. Rev. Lett. **105**, 162301 (2010); T. Lappi and H. Mantysaari, Nucl. Phys. **A908**, 51 (2013).

[36] J. Jalilian-Marian and A. H. Rezaeian, Phys. Rev. D **86**, 034016 (2012).

[37] A. H. Rezaeian, Phys. Rev. D **86**, 094016 (2012).

[38] A. Stasto, B.-W. Xiao, and D. Zaslavsky, Phys. Rev. D **86**, 014009 (2012).

[39] J. R. Ellis, M. K. Gaillard, and D. V. Nanopoulos, Nucl. Phys. **B106**, 292 (1976); M. A. Shifman, A. I. Vainshtein, M. B. Voloshin, and V. I. Zakharov, Yad. Fiz. **30**, 1368 (1979) [Sov. J. Nucl. Phys. **30**, 711 (1979)]; J. F. Gunion, P. Kalyniak, M. Soldate, and P. Galison, Phys. Rev. D **34**, 101 (1986); J. F. Gunion, G. L. Kane, and J. Wudka, Nucl. Phys. **B299**, 231 (1988).

[40] E. L. Berger, E. Braaten, and R. D. Field, Nucl. Phys. **B239**, 52 (1984); P. Aurenche, A. Douiri, R. Baier, M. Fontannaz, and D. Schiff, Z. Phys. C **29**, 459 (1985); D. A. Dicus and S. S. D. Willenbrock, Phys. Rev. D **37**, 1801 (1988); B. Bailey, J. F. Owens, and J. Ohnemus, Phys. Rev. D **46**, 2018 (1992); B. Bailey and J. F. Owens, Phys. Rev. D **47**, 2735 (1993); B. Bailey and D. Graudenz, Phys. Rev. D **49**, 1486 (1994); C. Balazs, E. L. Berger, S. Mrenna, and C.-P. Yuan, Phys. Rev. D **57**, 6934 (1998); C. Balazs and C.-P. Yuan, Phys. Rev. D **59**, 114007 (1999) , **63**, 059902 (2001); D. de Florian and Z. Kunszt, Phys. Lett. B **460**, 184 (1999); T. Binoth, J. P. Guillet, E. Pilon, and M. Werlen, Phys. Rev. D **63**, 114016 (2001); T. Binoth, arXiv:hep-ph/0005194; Z. Bern, A. De Freitas, and L. J. Dixon, J. High Energy Phys. 09 (2001) 037; C. Balazs, P. Nadolsky, C. Schmidt, and C.-P. Yuan, Phys. Lett. B **489**, 157 (2000); Z. Bern, L. J. Dixon, and C. Schmidt, Phys. Rev. D **66**, 074018 (2002); C. Anastasiou, K. Melnikov, and F. Petriello, Nucl. Phys. **B724**, 197 (2005); C. Balazs, E. L. Berger, P. M. Nadolsky, and C.-P. Yuan, Phys. Rev. D **76**, 013009 (2007); S. Catani, L. Cieri, D. de Florian, G. Ferrera, and M. Grazzini, Phys. Rev. Lett. **108**, 072001 (2012); M. Carena, I. Low, and C. E. M. Wagner, J. High Energy Phys. 08 (2012) 060.

[41] T. Binoth, J. P. Guillet, E. Pilon, and M. Werlen, Eur. Phys. J. C **16**, 311 (2000).

[42] G. Aad *et al.* (ATLAS Collaboration), Phys. Rev. Lett. **108**, 111803 (2012); **716**, 1 (2012); S. Chatrchyan *et al.* (CMS Collaboration), Phys. Lett. B **710**, 26 (2012).

[43] L. D. McLerran and R. Venugopalan, Phys. Rev. D **59**, 094002 (1999).

[44] F. Gelis and A. Peshier, Nucl. Phys. **A697**, 879 (2002); **A707**, 175 (2002).

[45] F. Gelis and J. Jalilian-Marian, Phys. Rev. D **66**, 014021 (2002).

[46] J. F. Owens, Rev. Mod. Phys. **59**, 465 (1987).

[47] R. Baier, A. H. Mueller, and D. Schiff, Nucl. Phys. **A741**, 358 (2004).

[48] B. Z. Kopeliovich, A. H. Rezaeian, H. J. Pirner, and I. Schmidt, Phys. Lett. B **653**, 210 (2007); Phys. Rev. D **77**, 034011 (2008); A. H. Rezaeian *et al.*, arXiv:0707.2040; B. Z. Kopeliovich, A. H. Rezaeian, and I. Schmidt, Nucl. Phys. **A807**, 61 (2008); M. A. Betemps and V. P. Goncalves, J. High Energy Phys. 09 (2008) 019; B. Z. Kopeliovich, E. Levin, A. H. Rezaeian, and I. Schmidt, Phys. Lett. B **675**, 190 (2009); M. V. T. Machado and C. B. Mariotto, Eur. Phys. J. C **61**, 871 (2009); A. H. Rezaeian and A. Schaefer, Phys. Rev. D **81**, 114032 (2010); M. A. Betemps and M. V. T. Machado; Phys. Rev. D **82**, 094025 (2010); S. Abreu *et al.*, J. Phys. G **35**, 054001 (2008).

[49] I. I. Balitsky, Phys. Rev. D **75**, 014001 (2007).

[50] Y. Kovchegov and H. Weigert, Nucl. Phys. **A784**, 188 (2007); E. Gardi, J. Kuokkanen, K. Rummukainen, and H. Weigert, Nucl. Phys. **A784**, 282 (2007); J. L. Albacete and Y. V. Kovchegov, Phys. Rev. D **75**, 125021 (2007).

[51] A. Adare *et al.* (PHENIX Collaboration), Phys. Rev. Lett. **107**, 172301 (2011); E. Braidot (STAR Collaboration), Nucl. Phys. **A854**, 168 (2011); Ph.D. thesis, Utrecht University, School of Physics [arXiv:1102.0931].

[52] A. Adare *et al.* (PHENIX Collaboration), Phys. Rev. C **80**, 024908 (2009).

[53] A. D. Martin, W. J. Stirling, R. S. Thorne, and G. Watt, Phys. Lett. B **652**, 292 (2007); Eur. Phys. J. C **63**, 189 (2009).

[54] E. L. Berger and J.-W. Qiu, Phys. Rev. D **44**, 2002 (1991); S. Catani, M. Fontannaz, J. P. Guillet, and E. Pilon, J. High Energy Phys. 05 (2002) 028; P. Aurenche, M. Fontannaz, J.-P. Guillet, E. Pilon, and M. Werlen, Phys. Rev. D **73**, 094007 (2006); D. d'Enterria and J. Rojo, Nucl. Phys. **B860**, 311 (2012).